4-40 GHz In-Phase/180° Out-of-Phase Power Dividers with Enhanced Isolation

Hadi Hijazi, Marc Le Roy, Raafat Lababidi, Denis Le Jeune, André Pérennec

4-40 GHz In-Phase/180° Out-of-Phase Power Dividers with Enhanced Isolation

Hadi Hijazi [1,2], Marc Le Roy [1], Raafat Lababidi [2], Denis Le Jeune [2], Andre Pérennec [1]
[1] Univ Brest (UBO), [2] ENSTA Bretagne, Lab-STICC, UMR 6285, CNRS, F-29200 Brest, France
hadi.hijazi@ensta-bretagne.org

***Abstract*—This paper demonstrates a single topology to implement ultra-wideband in-phase and 180° out-of-phase power dividers which will be dedicated for ultra-wideband frontends and balanced antenna systems that require a decent amount of isolation between ports. Both power dividers are formed of two couples of microstrip-to-slotline transitions terminated with radial stubs and then cascaded with a multisection Wilkinson power divider. A parametric study of the microstrip-to-slotline transition is performed to identify the main parameters' influence on its frequency response, followed by a full-wave optimization. Both power dividers are designed on RO4003C substrates and both have the same size of 22×38 mm^2. Simulation results show that the power dividers can operate between 4 and 40 GHz with less than 6 dB insertion loss and with small amplitude and phase imbalances between output ports. And most importantly, both devices have at least 20 dB of isolation between output ports over the entire bandwidth.**

Keywords—in-phase power divider, out-of-phase power divider, balun, multisection Wilkinson power divider, microstrip-to-slotline transition, ultra-wideband.

I. Introduction

An in-phase power divider is a 3-port device that divides an input signal into two output signals that are, ideally, equal in phase and in magnitude. On the other hand, a 180° out-of-phase power divider, also referred to as balun power divider, divides the input signal into two output signals that are, ideally, equal in magnitude and 180° out-of-phase. Both types of power dividers are greatly useful in many applications and systems, such as balanced antennas [1], antenna arrays' feeding and beam-forming networks [2], and the newly rising In-Band Full-Duplex (IBFD) technology [3]. Both types of power dividers are required by many systems that are sensitive to the imbalances between their different branches, thus, it is of great importance to have both types of power dividers with similar performance and behavior. Therefore, a single topology, 2-in-1 topology, that can be used either to provide in-phase or out-of-phase power division functions over a wide bandwidth is highly favorable.

Some works in the literature that demonstrated wideband 2-in-1 topologies were already carried out [4]-[6]. For example, in [4] a 16.5 – 40 GHz balun power divider topology is implemented using microstrip-to-coplanar waveguide (CPW) and microstrip-to-coplanar stripline (CPS) transitions. In this example, the balun topology is wideband and has an average isolation between output ports of 13 dB, but it suffers from relatively high phase and amplitude imbalances between output ports given as ± 1.1 dB and $\pm 8°$ respectively. In [5], CPW-slotline-microstrip power dividers are presented, both power dividers show amplitude and phase imbalance between output ports of ± 1 dB and $\pm 5°$ respectively over a 3 - 16 GHz bandwidth; however, they suffer from poor isolation (around 10 dB) at output ports. And in [6], microstrip-slotline-microstrip power dividers are proposed, the power dividers operate between 4 and 45 GHz, but with poor isolation and matching at output ports, and the amplitude and phase imbalances are ± 1 dB and $\pm 7°$ respectively. The poor matching and isolation between the output ports in [5] and [6] is a consequence of the fact that a 3-port device cannot be lossless, reciprocal and matched at all ports at the same time.

However, for any broadband application that utilizes an RF power divider, to function properly, the power divider must be ultra-wideband with minimum imbalances in phase and magnitude between output ports and with a good amount of isolation between them (≥ 20 dB), and preferably compact. Obviously, each one of the previously mentioned power dividers lacks at least one of these features. So, in this paper, a 2-in-1 power divider topology that achieves all the above-mentioned specifications is reported. The used topology is formed of two couples of microstrip-to-slotline transitions that are terminated with radial stubs and then cascaded with a conventional multisection Wilkinson power divider.

The paper is organized as follows: section II presents a brief introduction to microstrip-to-slotline transitions followed by a parametric study and depicts the final results of the optimized transition. Section III demonstrates a brief description of the methodology of designing a multisection Wilkinson power divider and shows its performance. Section IV shows the final topology and its S-parameters followed by a discussion of the results. Finally, section V concludes on the results and points to future enhancements.

II. Microstrip-to-Slotline Transition Theory and Parametric Analysis

A. Microstrip-to-Slotline Transition

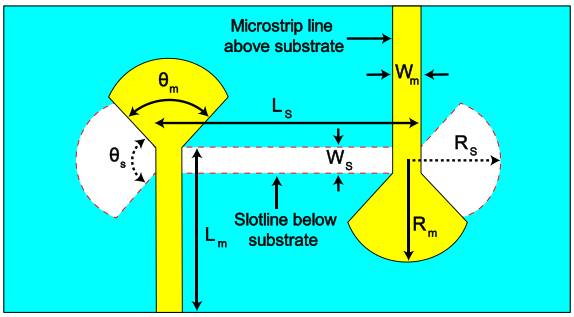

Fig 1. Microstrip-to-slotline transition as proposed in [7].

A microstrip-to-slotline transition is a planar structure that has a slotline etched in the ground plane and a microstrip line perpendicular to it etched on the top of the substrate. Both the slotline and the microstrip line are terminated by quarter-wavelength stubs that extend beyond the cross-junction. This configuration of transitions with straight quarter-wavelength is wideband in nature, however, its bandwidth can be greatly enhanced by replacing the straight quarter-wavelength stubs by radial stubs as depicted in Fig. 1. Indeed, it was shown by simulation that a transition with radial stubs has 28% extra bandwidth as compared to a transition terminated with straight quarter-wavelength stubs.

While it is easy to implement a 50 Ω microstrip line, it is very difficult to have a slotline with the same impedance for two reasons: first, due to slotline impedance dispersion with frequency, and second, realizing a low impedance slotline requires a very small slot width which could not be implemented using the available technology. Hence, usually, the slotline width -and consequently the slotline impedance- is altered to a realizable width causing some impedance mismatches between the microstrip line and the slotline. The available technology can generate a slotline with minimum slot width of 100 μm which corresponds to an impedance of 100 Ω at the center frequency (25 GHz). And to avoid the mismatch between the 50 Ω microstrip line and the 100 Ω slotline, the microstrip line could be tapered, however, the length of the taper will be significantly large at low frequencies, as a result, in this paper, the microstrip line was not tapered and kept at 50 Ω, then the simulations were carried out while considering this mismatch.

B. Parametric Analysis

Zinieris et al. [7] were the first to study a microstrip-to-slotline transition terminated with radial stubs. The proposed transition is formed of two microstrip-to-slotline transitions connected in a back-to-back configuration, as shown in Fig. 1. This configuration makes it microstrip-compatible at the input and output ports, and hence easier to implement, measure, and integrate with other microstrip devices. This transition was used as a benchmark for the performed parametric analysis, and it was reproduced in CST Microwave Studio (and dually checked in HFSS) with the initial parameters as in [7], then it was analyzed by varying individual parameters consecutively while fixing all other variables.

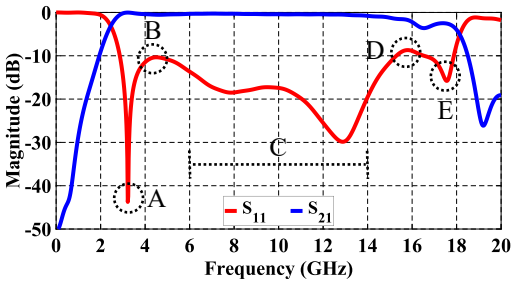

Fig. 2. Simulated s-parameters of the microstrip-to-slotline transition.

The simulated S-parameters of this transition with initial parameters and using lossless material are depicted in Fig. 2. Notice that the bandwidth is characterized by some specific points on S_{11} response: the position of the first local minimum (A), the level of the first local maximum (B), level of the last local maximum (D), position and level of the last local minimum (E) and the level of the in-band section (C) that is situated between the two local maxima. Usually, the in-band section level is controlled by the levels of its bounding maxima, therefore, by keeping their values as low as possible ensures that its level is also low. In order to obtain the widest bandwidth, the position of (A) should be shifted to the left of the frequency axis while decreasing the level of (B). In parallel, the position of (E) should be shifted to the right of the frequency axis, while maintaining its value and the (D) value at a low level.

The parametric analysis was dedicated to only study five parameters of the transition: the microstrip stub radius (R_m), the microstrip stub angle (θ_m), the slotline stub radius (R_s), the slotline stub angle (θ_s) and the slotline length (L_s). The microstrip line width (W_m) and the slotline width (W_s) were kept fixed as they correspond to fixed microstrip and slot impedances respectively and should not be altered.

TABLE I. SUMMARY OF PARAMETRIC ANALYSIS RESULTS

	A	B	C	D	E
R_m	–	↓	–	↖	↖
R_s	←	↖	–	↓	–
θ_m	–	↓	–	↓	–
θ_s	–	↑	–	↙	↙
L_s	↖	↖	–	↑	–

The results of the parametric analysis are illustrated in table I that shows how different parts of the bandwidth graph are affected by increasing each parameter. The leftmost column of the table shows the parameter being varied and the upper row shows the part of the bandwidth graph being affected (see Fig. 2). The dashes in the table tell that varying a specific parameter has no or negligible effect on a certain part of the bandwidth, while the arrow tells how and in which direction the curve will globally move if the parameter is increased. Also notice that different parts of the curve might be affected by multiple parameters, and sometimes are affected oppositely, so a good balance and a tradeoff between different parameters are needed to achieve the widest bandwidth possible.

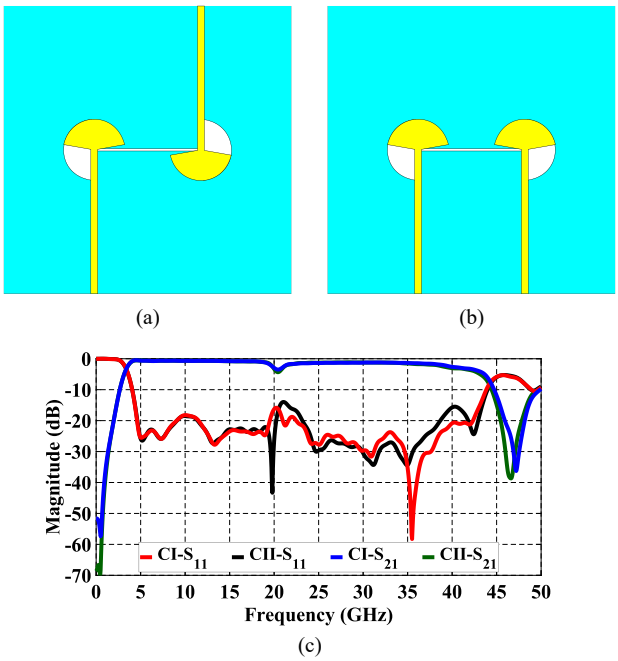

Fig 3. (a) Circuit I, (b) Circuit II and (c) their simulated S-parameters (In the legend they are abbreviated as CI and CII).

Based on the above observations, two microstrip-to-slotline transitions were designed and optimized on a RO4003C substrate (ε_r = 3.55) of thickness h = 203.2 µm. First, the transitions are tuned manually based on the results of table I and then are handed to the native optimizer. The two transitions are named Circuit I and Circuit II and they occupy an area of 18 × 18 mm^2. Basically, they have the same layout but their output microstrip lines are oriented oppositely. The purpose of the opposite orientation will be explained later in the paper. Fig. 3 depicts the simulated S-parameters of both transitions, using lossy metals and dielectrics, where it is

observed that both transitions operate in the frequency range between 4 and 43.8 GHz, with average insertion loss less than 1.5 dB over the entire bandwidth except at the upper edge of the bandwidth and in the area around 20.5 GHz. Notice how similar the S-parameters of both transitions are, this feature is the key for the sought-after 2-in-1 topology.

The insertion loss of the circuit drops at higher frequencies due to substrate dielectric losses and slotline radiation losses, but it is abnormal to drop around 20.5 GHz. The reason behind this drop is that the microstrip stub acts like a small patch antenna that radiates energy and resonates around 45 GHz, which is outside the band of operation. However, when the microstrip stub is mated with a slotline below it, it will act as a small patch antenna with a defected ground plane which results in changing the resonance frequency of the antenna to 20.5 GHz. Although the antenna is not perfectly matched at this frequency, the stub still radiates a decent amount of energy causing the dip in insertion loss. The solution to this problem will also be discussed later in this paper.

III. MULTISECTION WILKINSON POWER DIVIDER

It is possible to build wideband microstrip-to-slotline power dividers by using the optimized transitions as in [6]; however, they will be lacking isolation and matching at output ports, hence another power divider with good isolation and matching at output ports is needed. One of the most well known and most widely used power dividers is the Wilkinson power divider (WPD) [8], which has excellent return loss, insertion loss, and isolation at the center frequency. However, since this divider contains quarter-wave transmission lines, it only possesses less than 20% of fractional bandwidth, which renders it useless for wide-band applications.

TABLE II. INITIAL VALUES OF THE LINE IMPEDANCES AND RESISTOR VALUES OF THE POWER DIVIDER.

n	1	2	3	4	5	6
Z_n [Ω]	92.6	84.6	75.3	66.4	59.1	54
R_n [Ω]	120	120	200	315	500	675

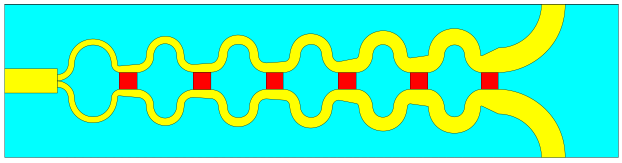

Fig. 4. Layout of the proposed 6-section Wilkinson power divider.

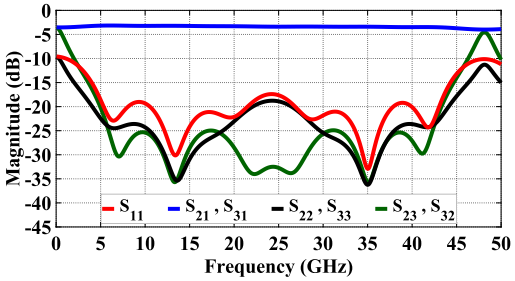

Fig. 5. Simulated S-parameters of the 6-section Wilkinson power divider.

In order to increase the bandwidth of operation of the WPD, Cohn [9] proposed to use a multi-section 2:1 impedance transformer with multiple isolation resistors placed between the two arms of each transformer section. The sections are quarter wavelength at the center frequency and are designed following the Chebyshev polynomials. By increasing the number of sections of the WPD the bandwidth is increased, however, this comes at the expense of an increased circuit size. Conventionally, the bandwidth of the WPD is measured in terms of isolation between output ports, and usually, a 20dB isolation level is the standard value. In this paper, a 6-section WPD is designed at a center frequency of 22.5 GHz, it provides around 142% of fractional bandwidth, thus, theoretically, covering the 5 – 40 GHz frequency range.

Based on [9] the impedance of each transformer section and its corresponding resistor value are calculated (Table II), then the initially obtained values are entered in a Keysight Advanced Design Systems (ADS) schematic using, firstly, ideal elements and optimizing the whole structure to squeeze out the maximum isolation over the design bandwidth. Next, another schematic of the WPD is built in ADS using microstrip transmission lines, and finally, the power divider is optimized again for the best results.

The procedure is then continued in the 3D simulator (CST) to study the effects of edge discontinuity and integrated resistors, and of course, to draw the final PCB layout. The layout of the proposed 6-section WPD is depicted in Fig. 4 and it was inspired by [10]. The proposed layout results from a trade-off between S-parameters responses, compactness, and ease of implementation of integrated resistors for the different desired resistance values. In addition to that, the integrated resistors were simulated as sheet resistances and resulted in an increased insertion loss at higher frequencies due to their big size as compared to the wavelengths at such frequencies. As a result, the dimensions of the resistors were reduced. Finally, the simulated S-parameters are depicted in Fig. 5.

IV. IN-PHASE/180° OUT-OF-PHASE POWER DIVIDERS DESIGN

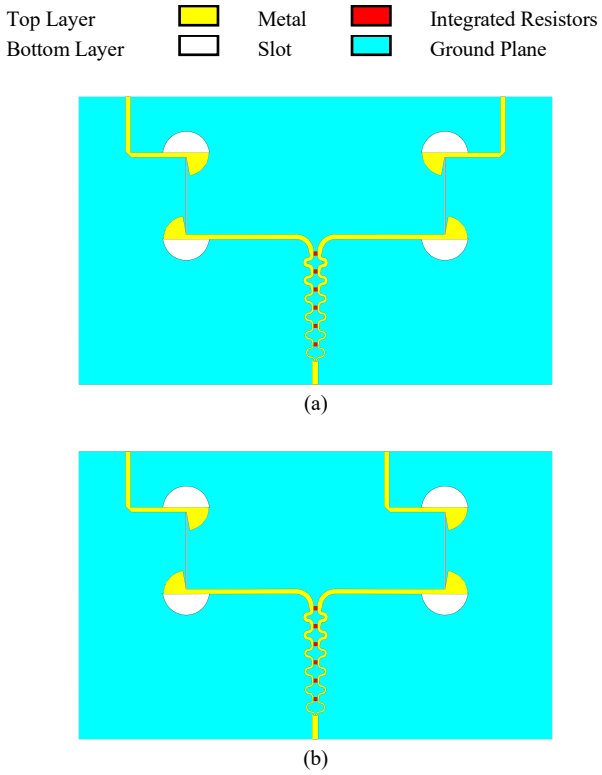

Fig. 6. The final 2-in-1 power divider topology, (a) in-phase power divider and (b) balun power divider.

To obtain an in-phase power divider, the WPD can be cascaded with either two Circuits I or two Circuits II, so that the output microstrip lines are symmetrical with regards to the central axis of the WPD (Fig. 5(a)). On the other hand, to obtain a balun power divider, the WPD can be cascaded with both Circuit I and Circuit II (Fig. 5(b)), since they have oppositely oriented output microstrip lines, then, a 180° phase shift between the output ports is introduced over the entire bandwidth. Now, a question arises: if an in-phase power divider is required, can't the 6-section WPD be used solely without the transitions? Doesn't adding the transitions to it seems meaningless and adds more losses and more radiation? In fact, this is true, adding the transitions to the WPD is not necessary for its in-phase power division function and adds losses and radiation to the system. However, the topology was designed for systems that require both types of power division (in-phase and 180° out-of-phase) at the same time with similar performance and behavior. Hence, if both a power divider balun and a WPD, without transitions at the outputs, are used in one system, this will cause more imbalances in magnitude and phase in different branches of the system.

The proposed topology in this paper may seem close to that of the reference in [11]. However, there are three major differences between both designs: first, in [11] the authors used a single section WPD, but of course, they are working on a different frequency range, yet the single section WPD didn't provide the required amount of isolation (20 dB) over the intended bandwidth. Second, in [11] the microstrip-to-slotline transitions were terminated with circular stubs, which were found to have a narrower bandwidth (but not narrow) than the radial stubs. And third, it was mentioned in section II-*B* that due to the overlap between the microstrip stubs and the slotline stubs the transition radiates more energy around 20.5 GHz and causes a dip in the insertion loss. Thus, the problem can be solved by eliminating the overlap between the two types of stubs, so for this reason, the microstrip stubs were cut in half as shown in Fig. 6. This eliminates the overlap; however, it directly affects the matching at the lower frequencies. Nevertheless, the degradation in matching does not severely affect the bandwidth of operation. This solution was inspired by [12].

For the sake of clearance and neatness of figures, only the simulated S-parameters of the balun power divider are depicted in Fig. 7. However, the in-phase power divider has approximately the same parameters as the balun, but it differs evidently in the phase imbalance between output ports which is 0° in this case. The whole circuit occupies an area of $22 \times 38\ mm^2$ and it operates between 4 and 40 GHz with insertion loss better than 6 dB (including the 3dB power division). The circuit shows a good matching at output ports and at least 20 dB of isolation between output ports. Finally, very small phase and amplitude imbalances were found between output ports in simulation.

Both circuits are currently under construction and measurements could be presented in the final version of this paper or during the conference. In addition to that, planar wideband antennas were designed and are currently being fabricated. The power dividers and the antennas will be used to implement a wideband full-duplex system based on [3].

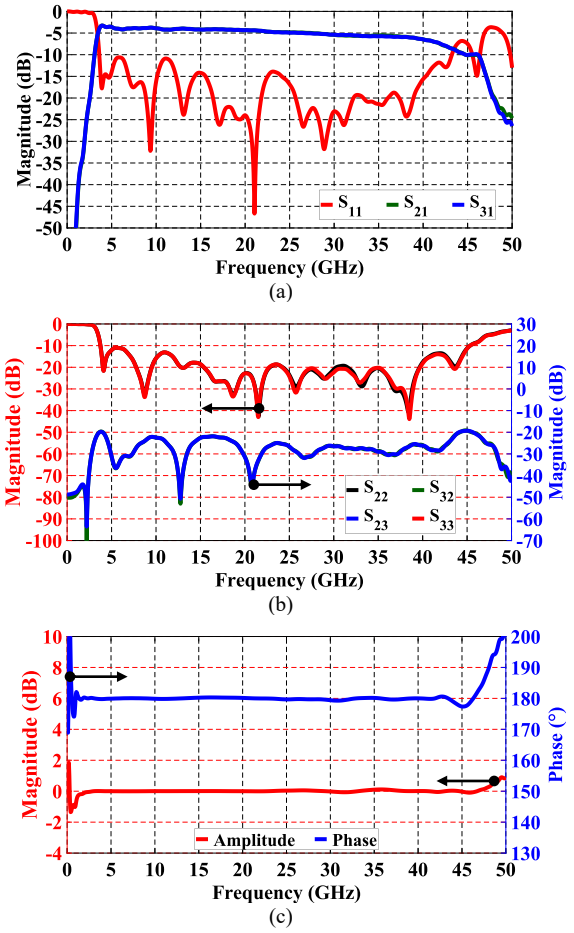

Fig. 7. Simulated S-parameters of the balun power divider: (a) input matching and insertion losses, (b) output ports' matching and isolation, and (c) phase and amplitude imbalances between output ports.

V. Conclusions and Perspectives

The proposed power divider topology is simple to design and to implement using basic PCB technology and a single dielectric layer. This 2-in-1 topology is most suitable to use in systems that require both in-phase and 180° out-of-phase power division with same performance and behavior. The ultra-wide bandwidth of the proposed power divider makes it beneficial for wideband systems such as radars, In-Band Full-Duplex, antenna arrays, etc. In addition to that, the power divider can be adapted to feed wideband slot antennas by adding single microstrip-to-slotline transitions at the power divider's outputs. On the other hand, the main drawback of this power divider topology is the leaking energy, mainly from the slotline, that might couple to adjacent components of the system and thus causes an unwanted interference, this can be avoided by designing an enclosure for the power dividers. Another approach focuses on designing new slotline stubs to limit the power radiation. A further enhancement to this device can be the modification of the shape and performance of the multisection Wilkinson power divider.

References

[1] S. Pegwal, M. P. Abegaonkar and S. K. Koul, "Ultrawideband doubly tapered slot antenna (DTSA) with integrated balun as a feed for time-domain target detection," Microwave and Optical Technology Letters, vol. 59, no. 10, October 2017, pp. 2415 – 2421.

[2] H. Zhu, H. Sun, C. Ding, and Y. J. Guo, "Butler Matrix Based Multi-Beam Base Station Antenna Array," In 2019 13th European Conference on Antennas and Propagation (EuCAP), IEEE, March 2019, pp. 1 – 4.

[3] E. Aryafar, M. A. Khojastepour, K. Sundaresan, S. Rangarajan and M. Chiang, “MIDU: Enabling MIMO Full Duplex,” In Proceedings of the 18th annual international conference on Mobile computing and networking, ACM, August 2012, pp. 257 – 268.

[4] P. Wu, Z. Wang and Y. Zhang, “Wideband planar balun using microstrip to CPW and microstrip to CPS transitions,” Electronics letters, vol. 46, no. 24, November 2010, pp. 1611 – 1613.

[5] A. K. Horestani and Z. Shaterian, “Ultra-wideband balun and power divider using coplanar waveguide to microstrip transitions,” AEU-International Journal of Electronics and Communications, vol. 95, October 2018, pp. 297 – 303.

[6] U. L. Rhode et al., “Ultra wide band balun/180° power divider using microstrip-slotline-microstrip transition,” In 2015 IEEE MTT-S International Microwave and RF Conference (IMaRC), IEEE, December 2015, pp. 400-404.

[7] M. M. Zinieris, R. Sloan, and L. E. Davis, “A broadband microstrip-to-slotline transition,” Zinieris, M. M., R. Sloan, and L. E. Davis. "A broadband microstrip‐to‐slot‐line transition." Microwave and Optical technology letters, vol. 18, no. 5, August 1998, pp. 339-342.

[8] J. E. Wilkinson, “An N-way hybrid power divider,” IRE Trans. on MTT, vol. 8, no. 1,1960, pp. 116 - 118.

[9] S. B . Cohn, “A class of broadband three-port TEM-mode hybrids,” IEEE Trans. on MTT, vol. 16, no. 2, Feb. 1968, pp. 110-116.

[10] B. Deutschmann and A. F. Jacob, “Compact ultra-broadband power dividers with integrated resistors,” In 2018 48th EuMC, September 2018, pp. 620-623.

[11] M. Bialkowski and Y. Wang, “UWB planar out-of-phase Wilkinson power divider utilizing UWB $\pm 90°$ phase shifters in microstrip-slot technology,” In APMC 2011, IEEE, December 2011, pp. 1138-1141.

[12] N. B. Wang, Y. C. Jiao, L. Zhang, Y. Song, and F. S. Zhang, “A simple low-loss broadband 1 – 14 GHz microstrip-to-slotline transition,” Microwave and Optical Technology Letters, vol. 51, no. 9, September 2009, pp. 2236-2239.